



ELSEVIER

Human Movement Science 19 (2000) 567–595

HUMAN
MOVEMENT
SCIENCE

www.elsevier.com/locate/humov

A gentle introduction to the dynamic set-point model of human postural control during perturbed stance

Tjeerd M.H. Dijkstra

Department of Psychology, The Ohio State University, 1885 Neil Avenue, Columbus, OH 43210–1222, USA

Abstract

Three models of increasing complexity to capture three observed phenomena of postural control are described. The first-order model mimics the increase in standard deviation of sway with eyes closed, but none of the other phenomena. The damped spring model captures both the increase in standard deviation of sway with eyes closed and the change from phase-lag to phase-lead with increasing frequency of oscillation of a visual surround. The final model, the dynamic set-point model, extends the damped spring model by a degree of freedom that reflects the observed slow drift in baseline. Under the assumption of a strong coupling to positional information, the dynamic set-point model predicts a dependence between natural frequency and position coupling constant of the damped spring model. It is shown that this prediction is borne out in data obtained from haptically perturbed stance but not in data obtained from visually perturbed stance. © 2000 Published by Elsevier Science B.V. All rights reserved.

PsycINFO classification: 2330; 2240

Keywords: Human postural sway; Balance control

E-mail address: dijkstra.1@osu.edu (T.M.H. Dijkstra).

1. Introduction

In this paper, I approach the sensory integration that takes place in controlling posture from a modelling perspective using tools from dynamical systems theory. My goal is to design a model that captures the observed relationships between postural control and sensory stimulation. The model does not reflect any of the neurophysiological or biomechanical underpinnings of postural control. This does not mean that these underpinnings are not important. In fact, the relationship between the dynamic set-point model and a simple biomechanical model based on an inverted pendulum are presented in a companion paper (Dijkstra, 2000). The strength of the models presented below lies in the way they include one of the central goals of the posture control system: how to integrate the cues that contribute to upright stance. The model is worked out in detail for the contributions of vision and light touch. However, I will focus on examples from visually perturbed stance, and occasionally use results from haptically perturbed stance.

The goal of the model is to capture the following observed phenomena of the influence of vision on posture.

1. During quiet stance, standard deviation of sway is generally more with eyes closed than with eyes open.
2. In the visually perturbed stance paradigm, sway is phase-locked to the oscillation of the visual surround (“visual puppet” behavior). Sway tends to phase-lag for low frequencies of oscillation of the visual surround and tends to phase-lead for high frequencies of oscillation. The transition frequency is around 0.2 Hz. The gain (ratio of amplitude of oscillation of visual surround to amplitude of postural response) is relatively constant for frequencies up to around 0.5 Hz.
3. In the perturbed stance paradigm, there is a postural response at the driving frequency of the surround and a low-frequency baseline drift.

The first phenomenon has been reported many times, e.g. by Edwards (1946), Paulus, Straube and Brandt (1984) and Dijkstra, Gielen and Melis (1992). An exception to the increase in standard deviation of sway with eyes closed has been reported by Collins and De Luca (1995). They find two groups of subjects, one of which shows an insignificant decrease in standard deviation of sway with eyes closed. This finding has been challenged by Riley, Wong, Mitra and Turvey (1997b) who did not find any evidence for two groups and found that standard deviation of sway increases with eyes closed. The second phenomenon was first documented by Lee and Lishman (1975) and later by

many others, e.g. van Asten, Gielen and Denier van der Gon (1988) and Dijkstra, Schöner and Gielen (1994a). The last phenomenon has not been studied as intensely as the others. It is reported in detail in Gurfinkel, Ivanenko, Levik and Babakova (1995) and is also present in the data of Dijkstra, Schöner, Giese and Gielen (1994b, Figs. 2–4) and Jeka, Schöner, Dijkstra, Ribeiro and Lackner (1997, Fig. 3).

In contrast to earlier papers on the dynamical systems approach to postural control, I will spell out the logic of my currently favored system – the dynamic set-point model – in great detail. In particular, I will explore simpler model structures and show them to be inadequate. The first model to be developed is a first-order dynamical system (see Fig. 1, left panel). This model can reflect the first phenomenon of increase in standard deviation of sway with eyes closed, but it cannot capture the other two phenomena. The second model is the damped spring model (see Fig. 1, middle panel) proposed by Schöner (1991). This model was designed to capture the first two phenomena listed above. It cannot deal with the baseline drift. The final model that I develop is the dynamic set-point model (see Fig. 1, right panel). It is a further development of the damped spring model but includes a degree of freedom to capture baseline drift. All three models are linear and thus I will use standard linear system analysis tools to analyze the behavior of each of them.

The current paper is part of a trilogy. In one paper (Dijkstra & Crowell, 2000), I present the dynamic set-point model and compare it with the pinned

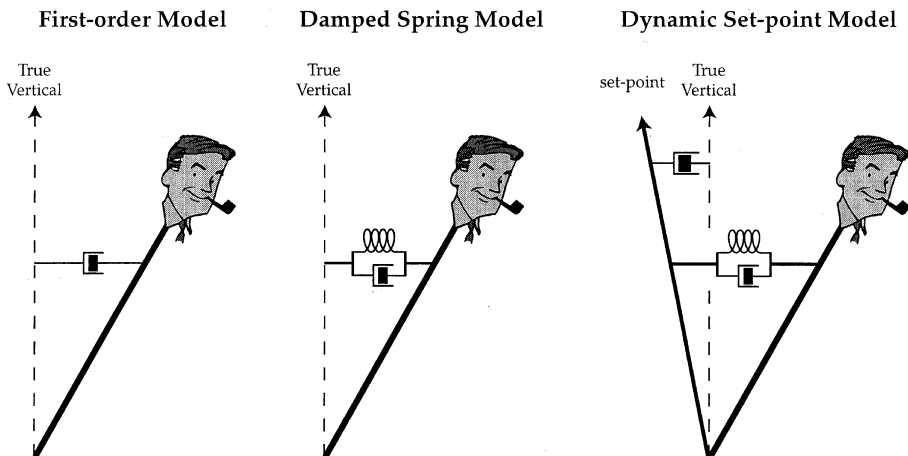


Fig. 1. Sketches of the structure of each of the models introduced below based on a mechanical analogy with springs for elastic forces and dashpots for viscous forces.

polymer model of postural control (Chow & Collins, 1995). I compare the models in terms of quality of fit of the autocovariance structure of a set of quiet standing data. I show that the pinned polymer model, the damped spring model and the dynamic set-point model all give a good account of the quiet standing data. In another paper (Dijkstra, 2000), I show how the center of pressure and center of mass dynamics can be biomechanically related in the context of the dynamic set-point model.

2. A first-order model of postural control

The second phenomenon – phase-lead for low frequencies and phase-lag for high frequencies – necessitates at least a second-order system. To make this point explicit, let us consider a simple first-order system. This simple system exhibits none of the three phenomena listed above but it highlights the choices made in designing the final system. A slightly more elaborate version of this model will be able to display the first phenomenon of increased standard deviation of sway with eyes closed. Furthermore, although it is not a good model of the control of upright posture, we will see below that this system does a good job of capturing the dynamics of the set-point. I denote the posture state (amplitude of sway) by x . This variable quantifies the deviation from upright in the forward/backward direction of the center of mass of the body. For simplicity, I take x to be a linear measure, not an angular one. I will denote the modulation of the position of the visual surround by s : in the experiments of Dijkstra et al. (1994a,b) s stands for the motion in depth of a fronto-parallel wall. In the examples below I will always use sine waves for s . I propose

$$\dot{x} = -\alpha_x x + c_p s. \quad (1)$$

This equation states that the change in posture state with respect to time (\dot{x}) is proportional to x with constant of proportionality α_x and proportional to s with constant of proportionality c_p . Taking both constants of proportionality positive leads to the desired behavior, for example, if the body has swayed forward ($x > 0$), then $-\alpha_x x$ is negative and thus the change in posture state \dot{x} is also negative, driving the posture state back to upright ($x = 0$). Similarly if the visual surround is moving forward ($s > 0$), then the change in posture state \dot{x} is positive and the posture state will move in the positive direction, i.e. sway forward. This is the visual puppet behavior, where the subject phase-locks to an oscillatory display. A numerical integration (Euler procedure with

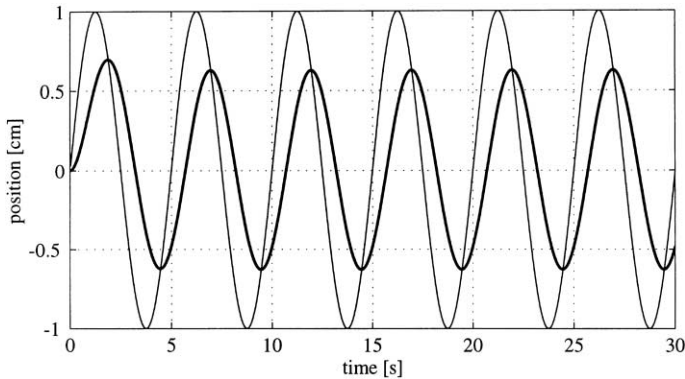


Fig. 2. Time series of first-order model (Eq. (1)) with parameters $\alpha_x = 1 \text{ second}^{-1}$ and $c_p = 1 \text{ second}^{-1}$. The stimulus s (thin line) is a sine wave with amplitude 1 and frequency 0.2 Hz, the response x (thick line) is a sine wave with amplitude 0.623 and frequency 0.2 Hz. The phase-lag of response relative to stimulus is -51.5° .

stepsize = 0.025 seconds) of Eq. (1) is shown in Fig. 2. Thus, the model seems in qualitative agreement with the second phenomenon, i.e. the posture state phase-locks to the motion of the visual surround.

I have introduced two parameters, α_x and c_p . Parameter α_x is the damping or friction constant. The name “damping” or “friction” derives from a mechanical analogy between physical forces and the dynamics of postural control, not from some physical damping in the joints. This term of the equation makes the system stable in the sense that after a perturbation, the system will return to a fixed state, $x = 0$. The larger the α_x , the faster the system recovers from a perturbation. Parameter c_p determines the strength of the influence of vision. Thus, the smaller this parameter the weaker the influence of s on the dynamics. In particular, $c_p = 0$ corresponds to eyes closed.

The system in Eq. (1) seems in qualitative agreement with the second phenomenon, in the sense that it displays phase-locking to a visual display. Does it also show the change from phase-lead to phase-lag as the frequency of the visual oscillation is increased? Unfortunately, this is where our simple system breaks down. In order to analyze its behavior, I calculate the transfer function, which is the Fourier transform of the posture state divided by the Fourier transform of the visual surround. The transfer function quantifies the relationship between the visual surround and posture state as a function of frequency. The calculation is performed in Appendix A and the result is plotted in Fig. 3. Since the transfer function is in general a complex function,

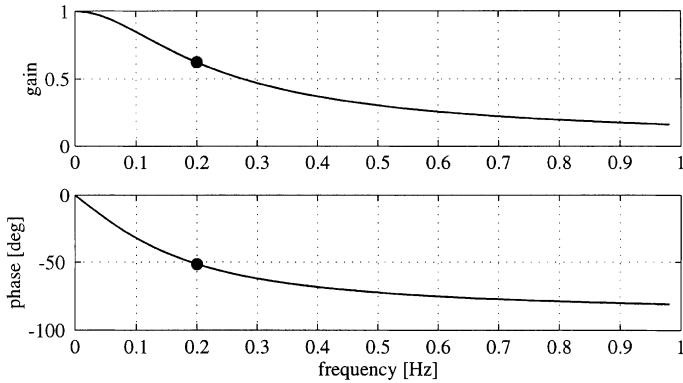


Fig. 3. Bode plots of the transfer function of the first-order model (Eq. (10)) with parameters $\alpha_x = 1 \text{ second}^{-1}$ and $c_p = 1 \text{ second}^{-1}$. Top panel – gain; bottom panel – phase difference between oscillation of visual surround and postural response as a function of frequency. The dot in both panels indicates the gain and phase for the data plotted in Fig. 2.

it is customary to plot it as a Bode plot, a pair of plots with one for gain and one for phase. The way to read a Bode plot is as follows: for a sinusoidal movement of the visual surround of 0.2 Hz and 1 cm (the stimulus in Fig. 2), the posture system responds with a sine wave with an amplitude of 0.623 cm and a phase-lag of -51.5° (the dots on the curves in Fig. 3). More generally, as shown in Appendix A, the phase-lag is always negative and it is impossible to choose parameters such that phase-lag is positive. Thus, our simple model of Eq. (1) is wrong.

The system of Eq. (1) is the simplest stable dynamical system in that it is linear and that it only contains a first-order derivative. Before we try a second-order system, let us try another approach. In our simple system, we coupled posture to the *position* of the visual surround. However, the posture control system might also couple to the *velocity* (denoted by \dot{s}) or *acceleration* (denoted by \ddot{s}) of the visual surround. Let us try a model with all three possible couplings. Also, from now on I will put all terms directly related to the posture state on the left-hand side and everything related to sensory input on the right-hand side. This is mainly for convenience since one can always transfer sides and add a minus sign.

$$\dot{x} + \alpha_x x = c_p s + c_v \dot{s} + c_a \ddot{s}, \quad (2)$$

where I have introduced c_v as the coupling constant of velocity and c_a as the coupling constant of acceleration. The transfer function of this system is calculated in Appendix B. How does the extended system of Eq. (2) deal with

the transition from phase-lead to phase-lag with increasing frequency? A typical example of a transfer function with only velocity coupling is shown in Fig. 4. Note that this system always phase-leads. Thus, it seems possible by combining position and velocity coupling to get both. Unfortunately, that is not the case. As shown in Appendix B, one still gets either phase-lead or phase-lag but not both. Adding acceleration coupling does allow both phase-lead and lag for different frequencies, for example for the values $\alpha_x = 1 \text{ second}^{-1}$, $c_p = -1 \text{ second}^{-1}$, $c_v = 2$ and $c_a = -1 \text{ second}$. However, as shown in Fig. 5, the gain is an ever increasing function of frequency, clearly different

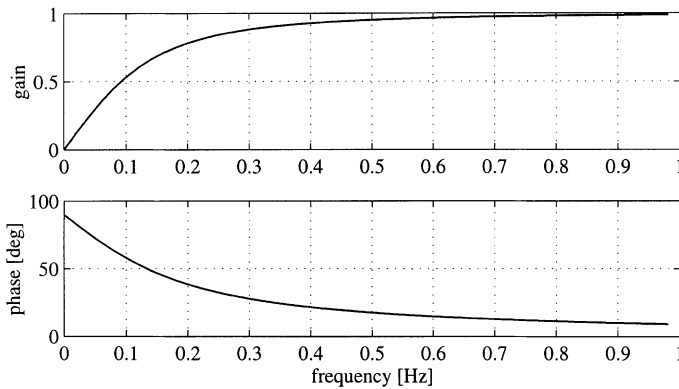


Fig. 4. Bode plots of first-order model (Eq. (2)) with parameters $\alpha_x = 1 \text{ second}^{-1}$, $c_v = 1 \text{ second}^{-2}$ and $c_p = c_a = 0$. Top panel – gain; bottom panel – phase difference between oscillation of visual surround and postural response as a function of frequency.

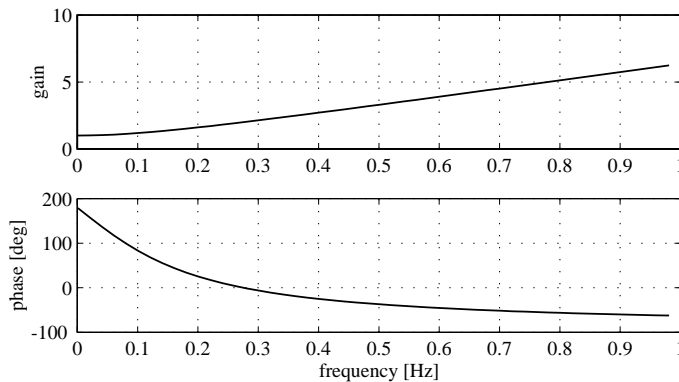


Fig. 5. Bode plots of first-order model (Eq. (2)) with parameters $\alpha_x = 1 \text{ second}^{-1}$, $c_p = -1 \text{ second}^{-1}$, $c_v = 2$ and $c_a = -1 \text{ second}$. Top panel – gain; bottom panel – phase difference between oscillation of visual surround and postural response as a function of frequency.

from the second phenomenon, where the gain is relatively constant for frequencies up to 0.5 Hz. In summary, it is impossible to extend the proposed first-order model by adding derivatives of the visual stimulation in order to make it show the observed behavior. As we will see below, adding a second derivative of the state variable (x) leads to the right behavior.

Ignoring the problem with the order of the system, how does it deal with the first phenomenon, of reduced standard deviation of sway with eyes closed? In order for the system to show spontaneous sway, we add a random perturbation to it, denoted by ξ_t . The characteristics of the random perturbation are determined by its statistical properties. For reasons of simplicity I choose zero-mean, unit variance, Gaussian white noise. “Zero-mean”, “unit variance” and “Gaussian” imply that the noise samples are drawn from a standard normal distribution. The whiteness of the noise implies that successive noise samples are uncorrelated, i.e. statistically independent. Making the variance of the noise an explicit parameter (denoted by Q_x), we arrive at the model

$$\dot{x} + \alpha_x x + \sqrt{Q_x} \xi_t = c_p s. \quad (3)$$

This equation (with stationary visual input, i.e. $s = 0$) was proposed by Newell, Slobounov, Slobounova and Molenaar (1997) as a model for the autocovariance structure of human postural control. If we take the visual input to be stationary, i.e. $s = 0$, the standard deviation of x in this model is given by (see Wang & Uhlenbeck, 1945, eq. (45))

$$\text{S.D.} = \sqrt{\frac{Q_x}{2\alpha_x}}.$$

This equation does not capture the reduction of S.D. with eyes closed since it does not depend on the visual coupling constant, c_p . However, by modifying Eq. (3) we can obtain a dependence that is qualitatively right. I have assumed that a non-zero influence of vision occurs for all non-zero values of s . Since the eye is attached to the body and thus moves with it, why not suppose that vision only exerts an influence when the *difference* between posture state and position of the visual surround is non-zero. Mathematically

$$\dot{x} + \alpha_x x + \sqrt{Q_x} \xi_t = c_p (s - x). \quad (4)$$

By taking the factor $c_p x$ over from the left-hand side to the right-hand side of this equation, we can see that the standard deviation of x in this model is given by:

$$\text{S.D.} = \sqrt{\frac{Q_x}{2(\alpha_x + c_p)}}.$$

Now the standard deviation depends on vision in the right way: the S.D. is reduced in the eyes open case as compared with the eyes closed case. This point is generally true: in order for a sensory contribution to reduce standard deviation of sway, one has to add the position specified by the sensor to the postural dynamics as a difference between posture state and position specified by the sensor.

The addition of noise to the dynamics brings about another way to think about the parameters α_x and c_p . One can think of the sum of them as fixing a time scale of interest for the variable x . The time scale is given by $1/(\alpha_x + c_p)$. Phenomena that occur on a much faster time scale are incorporated in the noise term ξ_t . One can make the separation between the variable of interest and the noise more explicit by positing many independent processes – not necessarily random – occurring on a faster time scale than that determined by $1/(\alpha_x + c_p)$. The addition of all these fast processes results in white noise.

3. Damped spring model of postural control

Having shown that a first-order model is inadequate to capture the second phenomenon, in particular the phase-lag for low and phase-lead for high frequencies combined with a relatively constant gain, I now turn to a second-order model. A second-order model allows for the possibility of specifying a natural frequency. This turns out to be critical in order to capture the second phenomenon. First, I rehash and discuss the assumptions of the damped spring model (Schöner, 1991). (1) The state of the postural control system is described by the position, x , of the center of mass in the forward–backward direction. (2) The posture control system generates a stable fixed point of this variable, at $x = 0$, $\dot{x} = 0$ by choice of coordinates. The dynamics of x is that of a second-order linear system. (3) Random fluctuations of upright posture are modeled as additive Gaussian white noise.

Before diving into the mathematics, let me discuss these choices. With respect to the choice of state variable, I have deviated slightly in taking the center of mass as the state variable; Schöner (1991) took the position of the center of the two eyes. This latter choice was dictated by convenience, since it was this position that was measured in the experimental papers (see Dijkstra

et al., 1994a,b) and because visual information is generally specified in these coordinates. Other than an amplitude difference (because the center of mass is about halfway up the body), there is no big difference between these two choices. For the relatively small amplitudes of motion considered here, the body generally moves as an inverted pendulum (Karlsson & Lanshammar, 1997).

The third choice – modeling fluctuations as additive Gaussian white noise – is dictated both by theoretical convenience and a time scale argument. The theoretical convenience stems from the fact that the power spectral density (PSD) can be calculated in closed form for all linear systems driven by white noise (see Gardiner, 1985). The PSD is defined as the squared absolute value of the Fourier transform of a certain time series. Intuitively, the PSD gives the power of the time series at each frequency (see Figs. 7 and 8 for a time series and its PSD). The time scale argument was introduced above. Briefly, if one assumes that there are many independent processes on a faster time scale than those explicitly being modeled, these processes can be modeled as additive Gaussian white noise. Thus, what is considered noise and what is considered part of the system dynamics is partly a matter of focus. Recently, there have been models of postural control in which non-white noise sources have been posited (e.g. Chow & Collins, 1995; Peterka, 1999) in conjunction with a second-order dynamics for upright. From my modeling standpoint, a degree of freedom with a time scale around 1 second has been ignored. In the dynamic set-point model described below, I capture this degree of freedom in a second variable u .

Another way in which fluctuations in motor control have been captured is through state-dependent noise. In this case the amplitude of the noise is not a constant but depends on the state of the dynamical system. For example Harris and Wolpert (1998) have proposed noise whose variance is proportional to the signal, like a Poisson process. In the present context, this would correspond to a variance proportional to the postural displacement. There is some evidence for this in the data of Riley, Mitra, Stoffregen and Turvey (1997a), who showed that the variance in the postural state is greater with the body leaned forward than upright. However, in this paper I will ignore these state-dependent effects. The reason for ignoring these is that I will calculate the experimental transfer function by averaging stimulus and postural response over at least one cycle of the stimulus oscillation. In that case one observes an average noise term over the cycle which can be described with a single constant, the noise power (denoted by Q_x).

A final point about noise is that white noise is physically impossible since it has finite power at infinitely high frequencies. In practice it is enough when the noise is white up to a certain frequency. In a companion paper (Dijkstra, 2000), I will show that the noise power is constant up to a frequency of 1.5 Hz, which is high enough to be treated as white.

Back to the meat, I propose

$$\ddot{x} + \alpha_x \dot{x} + \omega_0^2 x + \sqrt{Q_x} \zeta_t = c_v (\dot{s} - \dot{x}), \quad (5)$$

with parameters damping coefficient α_x , natural frequency ω_0 (in rad/second), coupling constant c_v and noise variance Q_x . Intuitively, the natural frequency (in Hz) of this oscillator is given by $f_0 = 2\pi\omega_0$ and the time it takes the posture system to regain equilibrium after a perturbation is given by $1/\alpha_x$. Parameter c_v determines the strength of the visual influence and Q_x determines the noisiness of the system. Similarly, as for the first-order model, x denotes the deviation from upright of the center of mass, and \dot{x} denotes its velocity. The acceleration of the center of mass is denoted by \ddot{x} and the velocity of the visual surround by \dot{s} .

This system has all the properties of the first-order model (Eq. (4)), displaying both the visual puppet behavior and the increase in standard deviation of sway with eyes closed. The visual puppet behavior is most easily understood by considering the case where the body is upright and motionless ($x = \dot{x} = 0$). In that case, forward motion of the visual surround ($\dot{s} > 0$) leads to a positive acceleration for the center of mass ($\ddot{x} > 0$) and vice versa for backward motion of the visual surround. The increase of standard deviation of sway follows from the enhanced damping by the $c_v \dot{x}$ term, in analogy with Eq. (4).

The version of the damped spring model proposed by Schöner (1991) contains a refinement of Eq. (5): the visual contribution to the posture control system is not the difference between stimulus velocity (\dot{s}) and rate of change of the posture state (\dot{x}) as it is in Eq. (5) (see also Schöner, Dijkstra & Jeka, 1998). Instead, the input is the expansion rate of a structure in the visual surround. For the stimulus used in the experimental papers (a moving fronto-parallel wall), this amounted to the difference between stimulus velocity and rate of change of the posture state divided by the distance to the wall. In Dijkstra et al. (1994a) we have shown the distance dependence to be necessary to explain the results of an experiment where the distance to a wall was varied. However, in the current paper I will only discuss the data of Dijkstra et al. (1994b) where distance was kept constant. Thus, I stick with the simpler version of the model in Eq. (5). A second advantage of writing the

model as Eq. (5) is that I can use the same model structure (with the addition of a position coupling term) to describe both the moving room and light touch paradigms.

How does this model stack up against the list of the three observed phenomena? With respect to phase and gain in the perturbed stance paradigm, it does quite well, as illustrated in Fig. 6. In this figure, I plot the observed gain and phase from an experiment on visually perturbed stance (thick line). Subjects were asked to stand relaxed and to look at a large screen (covering 110° field of view) on which a video image of a wall consisting of random dots was projected. The image oscillated in depth with a fixed frequency (0.05–0.5 Hz) and small amplitude such that the motion of the wall was barely detectable. See Dijkstra et al. (1994b) for a more detailed description of the methods. The gain and phase are the average of six trials for a single subject. Also plotted is a least squares fit of the transfer function of Eq. (5) (thin line). The functional form of the transfer function is derived in

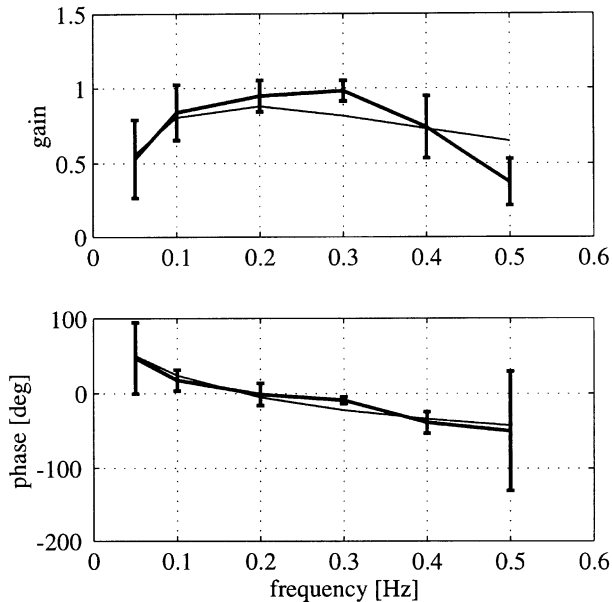


Fig. 6. Bode plots of the observed transfer function for a single subject in a visually perturbed stance paradigm (thick line). The errorbars denote the standard deviation across six repeats. Least squares fit with second-order model (Eq. (5)) with parameters $\alpha_x = 0.4 \text{ second}^{-1}$, $f_0 = 0.18 \text{ Hz}$ and $c_v = 2.6 \text{ second}^{-1}$ (thin line). Top panel – gain; bottom panel – phase difference between oscillation of visual surround and postural response as a function of frequency.

Appendix C. The least squares fit (using a Levenberg–Marquardt procedure, see Press, Flannery, Teukolsky & Vetterling, 1988) minimizes the norm of the difference between observed and model transfer function in the Gaussian plane. As can be seen in Fig. 6, the fit is quite satisfactory with a squared correlation coefficient between observed and fitted transfer function (R^2) of 0.93.

Similar fits of phase and gain were reported in Jeka, Oie, Schöner, Dijkstra and Henson (1998) for haptically perturbed stance. In the latter case, we found it necessary to include both a position coupling and a velocity coupling term into the dynamics. However, in the case of visually perturbed stance plotted in Fig. 6, it is not necessary to include a position coupling term. Of course, adding this term improved the fit but the model with position and velocity coupling has an extra parameter. One way to compare models with different numbers of parameters is through the Akaike information criterion or AIC (Myung, 2000), which we also used in Jeka et al. (1998). The AIC decreases as the proportion of variance explained increases but increases with the number of free parameters. The lower the AIC, the better the fit. For the data in Fig. 6, the AIC increases by adding position coupling. For the other six subjects in this experiment, three showed an increase and three a decrease in the AIC, making it unlikely that there is a significant contribution from visual position coupling in the moving room paradigm to control of sagittal posture.

Another way to illustrate the minor contribution of visual position information to the dynamics is by comparing the values of the fitted parameters (see Table 1). It is clear that the position coupling constant (c_p) is much larger in the light touch paradigm than in the moving room paradigm. Thus, it is unlikely that there is a large direct influence of position on the sagittal

Table 1

Results of fitting transfer functions of light touch and moving room data with a model with only velocity coupling or a model with both position and velocity coupling (see Eq. (18))^a

Paradigm	Coupling	α_v (second ⁻¹)	f_0 (Hz)	c_p (second ⁻²)	c_v (second ⁻¹)	R^2
Moving room	Velocity	2.4	0.21	N.A.	2.8	0.853
Moving room	Position and velocity	1.1	0.26	0.6	2.4	0.877
Light touch	Velocity	-0.9	0.21	N.A.	2.4	0.921
Light touch	Position and velocity	0	0.38	4.6	1.6	0.938

^aReported parameters are the average of six subjects for the light touch paradigm and seven for the moving room paradigm.

postural dynamics in visually perturbed stance. More support for this notion will be presented in Section 5.

The squared correlation coefficient between fitted and experimental transfer function (R^2) is generally high. The natural frequency is around 0.23 Hz for the visually perturbed stance paradigm (both types of model fits), and 0.38 Hz for the haptically perturbed stance paradigm fitted with a model with both position and velocity coupling. This might be due to the fact that the vision data pertain to sagittal motion and the haptic data to lateral motion. The fact that the damping coefficient is negative may seem strange at first blush. It means that the system needs the sensory input for stability. Similar effects have been observed before (Giese, Dijkstra, Schöner & Gielen, 1996) and are indicative of adaptive behavior.

With respect to the second phenomenon, the increase in standard deviation of sway with eyes closed, the picture is pretty much the same as for the first-order model. The standard deviation of x when the position of the visual surround (s) is constant is given by

$$\text{S.D.} = \sqrt{\frac{Q_x}{2\omega_0^2(\alpha_x + c_v)}}$$

This is identical to the standard deviation of the first-order model with the inclusion of a constant factor ω_0^2 . Thus, the damped spring model can capture the observed increase in standard deviation of sway with eyes closed.

Lastly, how does the model stack up against the third phenomenon, the baseline fluctuations? A plot of these fluctuations is given in Fig. 7 for a stimulus frequency of 0.3 Hz. An average PSD plot for this trial and five

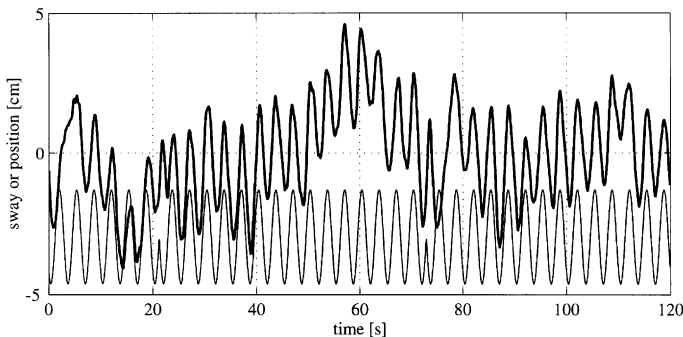


Fig. 7. Time series of stimulus (thin line) and response (thick line) in a visually perturbed stance paradigm. The stimulus has been shifted down for better viewing.

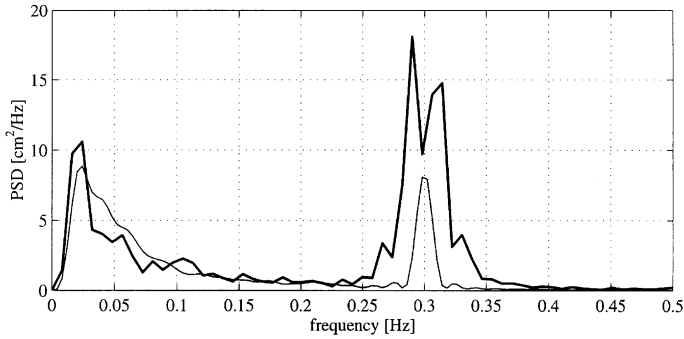


Fig. 8. PSD of postural sway in a visually perturbed stance paradigm (thick line). The split in the peak at 0.3 Hz is caused by the response to the 180° phase perturbations that occur around $t = 22$ seconds and $t = 75$ seconds in Fig. 7. The thin line is the PSD of a numerical integration of the dynamic set-point model (Eqs. (6) and (7)) with parameters $\alpha_x = 0.4 \text{ second}^{-1}$, $f_0 = 0.18 \text{ Hz}$, $Q_x = 5 \text{ cm}^2 \text{ second}^{-3}$, $\alpha_u = 0.2 \text{ second}^{-1}$, $Q_u = 0.5 \text{ cm}^2 \text{ second}^{-1}$, $c_x = 2.6 \text{ second}^{-1}$ and $c_u = 0 \text{ second}^{-1}$.

repeats is given in Fig. 8. One clearly observes a low-frequency component in the time series and a significant peak between 0.02 and 0.1 Hz in the PSD. Other examples of this low-frequency “rumble” are given in Jeka et al. (1997, Fig. 3). Unfortunately, the damped spring model cannot capture these baseline fluctuations. Since it is a linear system, it will only have significant power at the driving frequency and no power at any other frequencies. Thus, we need a more elaborated model structure to capture these fluctuations, which leads us to the dynamic set-point model.

4. Dynamic set-point model of postural control

The dynamic set-point model is an extension of the damped spring model. The extension is the addition of an extra degree of freedom (denoted by u) that captures the baseline fluctuations. I call this extra degree of freedom the set-point since it determines the stable point of the dynamics of x . I will refer to the dynamics of x as the dynamics of upright and to the dynamics of u as the set-point dynamics. I hypothesize the set-point dynamics to be first order and to couple to position, in the manner of the first-order model, Eq. (4). Explicitly:

$$\ddot{x} + \alpha_x \dot{x} + \omega_0^2(x - u) + \sqrt{Q_x} \zeta_t = c_x(\dot{s} - \dot{x}), \tag{6}$$

$$\dot{u} + \alpha_u u + \sqrt{Q_u} \zeta_t = c_u(s - u). \tag{7}$$

The first four parameters, damping coefficient α_x , natural frequency ω_0 , coupling constant c_x and noise variance Q_x , have the same meaning as for the damped spring model. The extra parameters of the dynamic set-point model are the damping coefficient α_u , noise power Q_u , and the coupling constant c_u , all of which have the same meaning as in Eq. (4). I will refer to c_x as the upright coupling constant and to c_u as the set-point coupling constant. Although c_x determines the strength with which velocity information couples into the dynamics of upright, I reserve the name velocity coupling constant for the constant c_v , that I introduced in Eq. (5). Similarly, I reserve the name position coupling constant for c_p . The reasons for this will become clear when I discuss the relationship between these two sets of parameters in Section 5.

The new contribution of this model is the set-point dynamics of Eq. (7). The set-point u is measured in the same coordinate system and units as x and thus can also be conceived as a deviation from the vertical. The concrete mathematical form chosen (a first-order system) should be regarded as a speculative. Below I give some evidence both from my own data and from a study by Gurfinkel et al. (1995) that the chosen form is consistent with older data. Beyond consistency, the first-order model is the simplest model in the sense of fewest parameters and order of differentiation.

How does the dynamic set-point model fare vis-à-vis the three phenomena? As usual, the response of the model is best characterized through the transfer function, which is calculated in Appendix D. In the appendix, I show that the transfer function of the dynamic set-point model reduces to the one of the damped spring model if we assume a small coupling constant (c_u) in the set-point dynamics. This seems a reasonable assumption since the observed transfer function reported in Fig. 6 pertains to forward/backward sway in the moving room paradigm and vision provides a weak position cue in this direction. Indirect evidence that the assumption holds will be provided in the next section. In summary, because the dynamic set-point model behaves like the damped spring model in this respect, we can say that the dynamic set-point model captures the observed gain and phase as well as the damped spring model, which did a good job.

How does the model do with respect to the increase in standard deviation of sway with eyes closed? Unfortunately, the expression for the standard deviation of the dynamic set-point model is quite long (see Dijkstra & Crowell, 2000, eq. (8) with $\tau = 0$). However, because the dynamic set-point model consists of two components (a first-order system and a damped spring system), both of which I have shown to exhibit the desired behavior, the dynamic set-point model itself also must show the increase in standard

deviation of sway with eyes closed. A second point relates to the fact that I choose to model the baseline fluctuations as an extra degree of freedom (denoted by u). Given the way the set-point dynamics couples into the dynamics of upright, it effectively injects low-pass filtered noise into the dynamics of upright. An alternative choice, made by Chow and Collins (1995) and Peterka (1999), is to posit low-pass filtered noise in the dynamics of upright (x dynamics) without the extra degree of freedom (u dynamics). With their choice, the noise sources are not white but structured. Below, I hope to convince the reader that the introduction of an extra degree of freedom (the set-point u) is the right choice for the postural control system.

Finally, how does the model fare with respect to baseline fluctuations? An example of baseline fluctuations is shown in Figs. 7 and 8. The last figure shows an observed PSD and a PSD obtained from a numerical integration (Euler integration with stepsize 0.015 second, see Zwillinger (1989, eq. 165.3)) of the dynamic set-point model. The parameters used in the simulation were mostly obtained from the fit of the transfer function plotted in Fig. 6. In particular, the values for $\alpha_x = 0.4 \text{ second}^{-1}$, $f_0 = 0.18 \text{ Hz}$ and $c_x = 2.6 \text{ second}^{-2}$ were obtained from the transfer function fit. Parameter c_u was set to zero and Q_x was set to $5 \text{ cm}^2 \text{ second}^{-3}$. The quality of the fit depended very weakly on the latter value. Parameters $\alpha_u = 0.2 \text{ second}^{-1}$ and $Q_u = 0.5 \text{ cm}^2 \text{ second}^{-1}$ were the only free parameters and were adjusted by hand so as to match the peak between 0.02 and 0.1 Hz. As one can see, the model gives a fairly good fit to the data. The only aspect of the fit that is not so good is the height of the peak at 0.3 Hz: the model gives a value for the gain that is too low. However, as can be seen in Fig. 6, the gain at 0.3 Hz is already too low in the transfer function fit. One way to increase the quality of the fit would be to increase the parameter c_x . This would increase the influence of the visual perturbation which would increase the amplitude of x at the frequency of the visual perturbation. However, in doing so one would lose the elegance of the current fit, in which only two parameters are free. In summary, the dynamic set-point model exhibits all three observed phenomena in a relatively simple dynamical system.

5. Dynamics of set-point: A reinterpretation of the light touch paradigm and moving room paradigm

Further evidence in favor of the dynamic set-point model comes from the light touch paradigm and moving room paradigms. In the first paradigm,

subjects are asked to touch a touchbar with their finger. Subjects stand in a heel to toe posture and the lateral excursion of their center of mass is recorded. The touchbar is moved in an oscillatory fashion, which induces a postural response in the subject. In Jeka et al. (1998), we introduced a variant of the damped spring model in order to account for the observed transfer functions. It was necessary to include both position and velocity coupling in order to obtain satisfactory fits of the observed transfer functions. Mathematically, we proposed

$$\ddot{x} + \alpha_x \dot{x} + \omega_0^2(x - y) + \sqrt{Q_x} \xi_t = c_v(\dot{s} - \dot{x}) + c_p s, \quad (8)$$

with position coupling strength c_p and velocity coupling strength c_v . Note that s now stands for the motion of the touchbar. Since the model structures for moving room and light touch paradigms are the same, I do not introduce special symbols for the different types of stimulation. In the sequel I will show that the dynamic set-point model predicts a dependence between the parameters of the model used to fit the data of Jeka et al. (1998). To this end I relate the coupling parameters of this model to the parameters c_x and c_u of the dynamic set-point model. It is shown in Appendix E that the velocity coupling constant (c_v) is equivalent to the upright coupling constant (c_x). The relationship between the position coupling constant (c_p) and the set-point coupling constant (c_u) is more complex. However, when one assumes that parameter c_u is large one can simplify the relationship between c_p and c_u . Mathematically, if we take $c_u \gg \omega$ and $c_u \gg \alpha_y$ we get

$$c_p \approx \frac{c_u \omega_0^2}{c_u} = \omega_0^2. \quad (9)$$

This leads to a verifiable prediction: if the dynamic set-point model is correct and if parameter c_u is relatively large, then the position coupling constant and the squared natural frequency calculated by fitting the transfer function of Eq. (9) (see Eq. (18)) to the observed transfer function should be equal. This relationship is plotted in Fig. 9 for the six subjects of Jeka et al. (1998). Each data point is obtained from a fit of the theoretical transfer function of Eq. (18) to experimentally observed transfer functions. The observed transfer functions were calculated from five trials for stimulus frequencies 0.1, 0.2, 0.4, 0.6 and 0.8 Hz. The fits provide a c_p – ω_0 pair for each fitted transfer function. The slope and intercept of the regression of ω_0^2 on c_p is tabulated in Table 2. As one can see there is scatter in the slopes but each observed slope includes the predicted slope of 1.0 within a 95% confidence interval, but the scatter in the intercepts does not generally include the predicted value of zero.

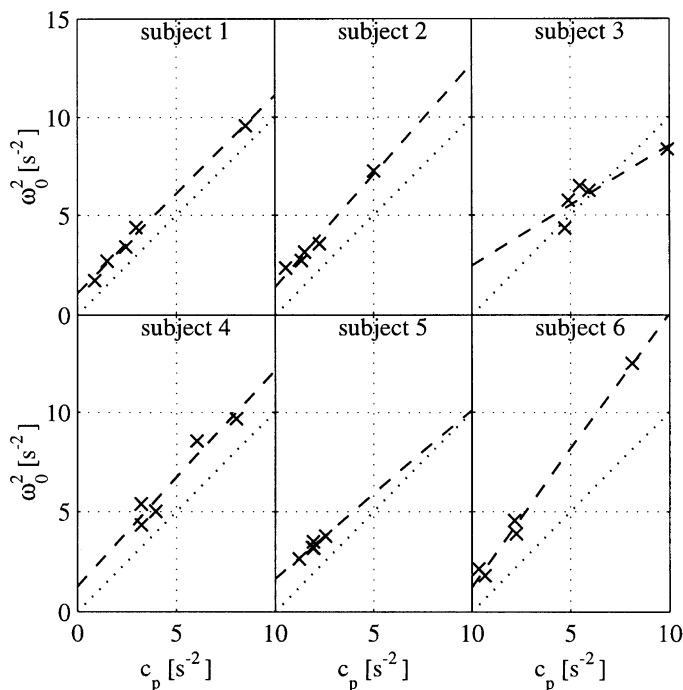


Fig. 9. Plot of parameter ω_0^2 versus c_p for six subjects. Indicated are the best fitting line from a linear regression and the diagonal, i.e. the prediction from Eq. (9).

Table 2
Light touch data^a

Subject	Slope	Intercept	R^2	P
1	1.00 ± 0.14	1.09 ± 0.56	0.995	0.0002
2	1.13 ± 0.31	1.40 ± 0.81	0.978	0.0014
3	0.61 ± 0.55	2.48 ± 3.53	0.808	0.0380
4	1.09 ± 0.53	1.27 ± 2.78	0.934	0.0073
5	0.85 ± 0.48	1.65 ± 0.93	0.915	0.0109
6	1.38 ± 0.23	1.24 ± 0.90	0.992	0.0003

^aSlopes, intercepts, squared correlation coefficients (R^2) and significance (P) of the linear regressions plotted in Fig. 9. Slopes and intercepts are given with 95% confidence intervals.

Unfortunately, the experiment was not designed in a block random fashion but in a completely random design. With a block random design, the different frequency conditions needed to fit a single transfer function would be as close in time as possible and changes of the system parameters within a block would be less likely. In order to obtain the observed transfer functions,

I have grouped the first repeat of every condition in the first group, the second repeat in the second group etc. Thus, what we observe in Fig. 9 is a covariation between parameters from group to group, on a time scale of around 10 minutes (each trial lasted 90 seconds with about 30 seconds break between trials). One can do a similar analysis by fitting the average transfer function (across groups) of a subject and one obtains a c_p - ω_0 pair for each subject. A regression of ω_0^2 on c_p leads to a slope of 0.74 ± 0.39 and an intercept of 2.04 ± 1.50 . Thus, the between-subjects results are similar to the within-subject results. In both analyses the confidence limits of the intercept usually do not include zero, contrary to the prediction of Eq. (9). However, the intercept is always positive which is supported by the following reasoning. The natural frequency cannot become zero or the postural control system is unstable. In contrast, the position coupling constant can become zero or even negative without it becoming unstable.

In order to illustrate that the regression of ω_0^2 on c_p is not necessarily significant for every data set from postural control, I analyze the data from the visual perturbed stance paradigm in a similar way. I showed above that adding position coupling was of little help in improving the transfer function fits of the moving room data. Applying the preceding analysis to these data provides further support for this result. It is reasonable to suppose that touch provides a stronger positional reference for lateral control of posture than vision does for sagittal control of posture. The argument in support of this is based on the fact that the greatest change in position for forward/backward motion of the head takes place in the visual periphery, where thresholds of detecting change in position are high. Thus, we expect no equality of ω_0^2 and c_p as derived from fits of observed transfer functions from the moving room paradigm. I performed the same analysis for the moving room data of Dijkstra et al. (1994b) as reported in Fig. 9 and Table 2. The observed transfer functions were generated in the same fashion as for the light touch paradigm. I grouped the data at each of the five stimulus frequencies (0.1, 0.2, 0.3, 0.4 and 0.5 Hz) and fitted the transfer function of Eq. (9) (see Eq. (18)) with both position and velocity coupling to each observed transfer function. I have shown above that these fits are not warranted in many of the subjects (since the AIC increases for four out of the seven subjects), but I ignore that here. The result of a regression of ω_0^2 on c_p for each subject is given in Table 3. In contrast to the data in Table 2, there is now only one subject for whom the fit is significant (according to the P -value) and the slope includes 1 within a 95% confidence interval. The same negative result emerges when we do a between-subjects regression. The R^2 is 0.053 and thus the fit is not significant.

Table 3
Moving room data^a

Subject	Slope	Intercept	R^2	P
1	19.47 ± 5.73	1.91 ± 0.35	0.957	0.0007
2	-13.38 ± 97.59	2.64 ± 2.23	0.035	0.7229
3	1.61 ± 0.54	1.23 ± 0.69	0.945	0.0011
4	2.17 ± 0.96	1.03 ± 0.49	0.908	0.0032
5	5.57 ± 5.00	2.13 ± 1.59	0.705	0.0365
6	0.74 ± 0.24	1.77 ± 0.91	0.947	0.0011
7	1.15 ± 0.18	0.52 ± 0.63	0.988	0.0001

^aSlopes, intercepts, squared correlation coefficients (R^2) and significance (P) of the linear regressions of ω_0^2 on c_p . Slopes and intercepts are given with 95% confidence intervals.

We can conclude by saying that vision indeed provides a weaker positional referent for sagittal sway than touch does for lateral sway. Second, we have shown that the observed parametric dependence between natural frequency and position coupling constant in the light touch paradigm is not a general feature of all data sets obtained from postural control.

We can summarize the reanalysis of the light touch data of Jeka et al. (1998) by saying that the dynamic set-point model predicts a relationship between two parameters of the position–velocity model they employed. Under the assumption that the set-point coupling constant is large, the dynamic set-point model predicts a linear dependence with slope one between position coupling constant and squared natural frequency. By fitting these parameters to observed transfer functions, we showed that this prediction is indeed reflected in the data. This shows the dynamic set-point model to be able to expose an undesired feature of the damped spring model with position–velocity coupling, viz. a linear dependence between its parameters. Thus, the dynamic set-point model captures the observed transfer functions from both haptically and visually perturbed stance without a parametric dependence. The assumption of strong coupling to static information seems plausible for haptic information but not for visual information with respect to the forward/backward direction. Thus, we would expect the set-point coupling constant to visual information to be relatively small. In that case the dynamic set-point model does not predict a linear dependence between position coupling constant and squared natural frequency. By performing similar fits to observed transfer functions, I showed the dependence to be different from the prediction. Although it is dangerous to draw a strong conclusions from a negative result alone, I believe the combination of both results to lend considerable support to the dynamic set-point model.

6. Discussion

I have introduced three models of increasing complexity to capture three observed phenomena of postural control. The first-order model could mimic the increase in standard deviation of sway with eyes closed, but none of the other phenomena. The damped spring model captured both the increase in standard deviation of sway with eyes closed and the change from phase-lag to phase-lead with increasing frequency of oscillation of a visual surround. The final model, the dynamic set-point model, extends the damped spring model by a degree of freedom that reflects the observed slow drift in baseline.

There have been suggested several models in the literature on postural control that propose two (or more) levels for the postural control system. A distinction between the contributions of static and dynamic visual cues to postural control was made by Amblard, Crémieux, Marchand and Carblanc (1985). By using stroboscopic illumination of a stationary wall, they showed two modes of visual control of lateral balance. A static mechanism operates below 2 Hz and is strobe resistant, and a dynamic mechanism which operates above 4 Hz and is not strobe resistant. Although the distinction between static and dynamic visual cues is closely related to my distinction of position and velocity cues, there is a big difference in time scales. In particular, the position cues that I included in the dynamic set-point model operate on a time scale of 5 seconds, around 0.2 Hz. Similarly, the velocity cues operate on a time scale of 0.5 seconds, around 2 Hz. Both of these are considerably different from the frequencies of the static and dynamic cues posited by Amblard et al. (1985). The cause of the relatively high frequency responses observed by Amblard et al. (1985) is more likely to be of a physiological origin and less related to the cue-integration problem addressed by the dynamic set-point model.

One proposal originates from Collins and De Luca (1993). They propose two time scales to explain the observed autocovariance structure of center of pressure data obtained during quiet standing. In a companion paper (Dijkstra & Crowell, 2000), we show that the dynamic set-point model is capable of capturing the observed autocovariance structure. Roughly, the two time scales observed by Collins and De Luca are mapped onto the damping coefficients (α_x and α_{ii}). By taking different values for the damping coefficients, the observed autocovariance structure emerges. Beyond capturing the two time scale finding of quiet stance, the dynamic set-point model includes the low-frequency drift and coupling to visual and haptic information during perturbed stance.

Recently, Zatsiorsky and Duarte (2000) proposed a decomposition of center-of-pressure trajectories into two components that they termed rambling and trembling. Rambling is the stochastic motion of the instantaneous equilibrium point and trembling the stochastic motion around that point. Instantaneous equilibrium points are those points in time where the horizontal force exerted by the subject equals zero. The rambling trajectory was obtained by a spline interpolation of these instantaneous equilibrium points and the trembling trajectory was the difference between the recorded center of pressure trajectory and the rambling trajectory. Thus, the PSD of rambling peaks at lower frequencies than the PSD of trembling. Zatsiorsky and Duarte found the rambling peak to lie at 0.16 Hz and the trembling peak at 0.57 Hz. Furthermore, the rambling peak is around 10 times higher than the trembling peak. It is tempting to view the dynamic set-point model as equivalent to the rambling–trembling decomposition. In that case the dynamics of upright equals the trembling part and the set-point dynamics, the rambling part. Since the rambling–trembling decomposition applies to quiet stance, I cannot use perturbed stance data to support or reject this identification. In a companion paper (Dijkstra & Crowell, 2000), where we analyze quiet stance data, we show that this identification is unlikely. Furthermore, in a second paper (Dijkstra, 2000), I give a possible explanation for the rambling–trembling decomposition. The explanation is based on the relation between stochastic center of pressure and center of mass dynamics under the assumption of inverted pendulum dynamics.

The set-point dynamics has been introduced as an extension of the damped spring model. Besides its success for the light touch and moving room paradigms, is there any other evidence for a set-point dynamics? Lestienne and Gurfinkel (1988) introduced a two-level control scheme for postural control. They described a low-level controller termed “operative” that achieves postural stability relative to a reference point and a high-level controller termed “conservative” that determines the reference point. Gurfinkel et al. (1995) tested this two-level scheme for postural control. They had subjects stand on a very slowly rotating platform and noticed that posture was stabilized around a slowly changing reference point. Thus, subjects did not stabilize their posture around a fixed reference point like the direction of gravity. It is not the case that they were incapable of stabilizing their posture relative to a fixed reference: when explicit feedback about posture was provided on an oscilloscope, subjects aligned their posture with the gravitational vertical. Thus it is tempting to identify the operative level with the x dynamics and the conservative level with the u dynamics of the dynamic set-point model.

A critical step in this identification is if the time scales that Gurfinkel et al. (1995) observed in their data match the values of α_u that I obtained in the fits. In one experiment Gurfinkel et al. (1995) used frequencies of platform oscillation of 0.003–0.017 Hz with amplitudes of 1.5° and observed phase-lags between platform rotation and body orientation in the range of 30–60°. Converting these values to time scales¹ leads to values in the range of 5–40 seconds. In a second experiment, Gurfinkel et al. (1995) used ramps of platform rotation of amplitudes 0.25° and 1° and constant rate of rotation of 0.04°/second. In this case they observed an initial period of fast change in body tilt that lasted around 3–5 seconds followed by a period of slow body change that lasted until the end of a trial. After the ramp was switched off, it took subjects around 20 seconds to reach a stationary state which was often not the same as the initial one. Converting these numbers to time scales of an exponential relaxation and assuming that about two relaxation times of this exponent can be observed, I estimate the time scales to be around 1–2 seconds for the ramp-on and around 10 seconds for the ramp-off case. Both experiments show that one cannot ascribe a single time scale to the conservative process and that it might itself consist of sublevels. Ignoring this subtlety for now, how do the ranges of time scales compare? In Fig. 8, I use a value of 0.2 second⁻¹ for α_u which equals a time scale of 5 seconds. This value falls squarely within the range observed by Gurfinkel et al. (1995), adding support to the idea of two-level control in posture. This hypothesis meshes nicely with the notion of Gurfinkel et al. (1995, p. 241) that “... the reference for the maintenance of vertical posture is constructed on the basis of multiple sources and is not based on a single parameter or sensory input”. An explicit mathematical model of this was presented in Eqs. (6) and (7). Thus, another way of viewing the set-point dynamics is a way to integrate sensory information from various modalities about the vertical, a point that has recently received considerable impetus in robotics (Steinhage & Schöner, 1997).

Acknowledgements

This work was supported by the National Science Foundation grant SBR-9809447 and by a seed grant from the Ohio State University. Discussions

¹ Denoting the frequency of stimulation by f_g , the phase-lag as ϕ_g (in radians) and the timescale as τ_g , the conversion is performed by $\tau_g = \arctan(\phi_g)/2\pi f_g$.

with Gregor Schöner were very helpful in formulating these ideas. Jim Crowell provided invaluable input in presenting the ideas and designed Fig. 1. The dynamic set-point model was first presented at the Annual Meeting of the Society for Neuroscience in November 1998. Last but not the least, I thank the Santa Fe Institute for supporting Dagmar's Dynamics Debates and Dagmar Sternad for moral support.

Appendix A

In this appendix, I calculate the transfer function of Eq. (1). The Fourier transform $X(\omega)$ of a time series $x(t)$ is defined by

$$X(\omega) = \int_{-\infty}^{\infty} x(t)e^{i\omega t} dt.$$

Transforming Eq. (1) leads to

$$i\omega X = -\alpha_x X + c_p S,$$

where I have used the fact that differentiation in the time domain corresponds to multiplication with $i\omega$ in the Fourier domain; see Kamen and Heck (1997, p. 177). The transfer function is now given by

$$T_{xs}(\omega) \equiv \frac{X}{S} = \frac{c_p}{i\omega + \alpha_x}. \quad (10)$$

The gain is the magnitude of the transfer function and the phase is its angle in the complex plane. Explicitly:

$$\text{gain} = \frac{c_p}{\sqrt{\omega^2 + \alpha_x^2}}, \quad (11)$$

$$\text{phase} = -\arctan\left(\frac{\omega}{\alpha_x}\right). \quad (12)$$

In particular, the phase is always negative when α_x is positive.

Appendix B

In this appendix, I calculate the transfer function of Eq. (2). Transforming Eq. (2) leads to

$$i\omega X + \alpha_x X = c_p S + c_v i\omega S - c_a \omega^2 S.$$

The transfer function is now given by

$$T_{xs}(\omega) \equiv \frac{X}{S} = \frac{c_p + i\omega c_v - \omega^2 c_a}{i\omega + \alpha_x}. \quad (13)$$

The gain is the magnitude of the transfer function and the phase is its angle in the complex plane. Explicitly:

$$\text{gain} = \frac{\sqrt{\omega^2(c_p - \alpha_x c_v - c_a \omega^2)^2 + (\alpha_x c_p + (c_v - c_a \alpha_x) \omega^2)^2}}{\omega^2 + \alpha_x^2}, \quad (14)$$

$$\text{phase} = \arctan \left(\frac{\omega(-c_p + \alpha_x c_v + c_a \omega^2)}{\alpha_x c_p + (c_v - c_a \alpha_x) \omega^2} \right). \quad (15)$$

In particular, when $c_a = 0$ the sign of the phase is determined by $-c_p + \alpha_x c_v$. When this factor is negative, so is the phase for all frequencies; when it is positive, so is the phase. Thus, when $c_a = 0$ it is impossible to have a phase transition from phase-lead to phase-lag for increasing frequency.

Appendix C

In this appendix, I calculate the transfer function of the deterministic part of the damped spring model (Eq. (5)). For an intuitive derivation of the following result see Feynman, Leighton and Sands (1963, vol. 1, chapters 21–25). Setting $Q_x = 0$ and Fourier transforming leads to

$$-\omega^2 X + \alpha_x i\omega X + \omega_0^2 X = c_x i\omega(S - X).$$

The transfer function is now given by

$$T_{xs}(\omega) \equiv \frac{X}{S} = \frac{i\omega c_x}{-\omega^2 + i\omega(\alpha_x + c_x) + \omega_0^2}. \quad (16)$$

Appendix D

In this appendix, I calculate the transfer function of the deterministic part of the dynamic set-point model (Eqs. (6) and (7)). Setting $Q_x = 0$ and Fourier transforming leads to

$$-\omega^2 X + \alpha_x i\omega X + \omega_0^2(X - U) = c_x i\omega(S - X),$$

$$i\omega U + \alpha_u U = c_u(S - U).$$

After some algebra, I find for the transfer function

$$T_{xs}(\omega) \equiv \frac{X}{S} = \frac{(c_u \omega_0^2) / (i\omega + \alpha_u + c_u) + i\omega c_x}{-\omega^2 + i\omega(\alpha_x + c_x) + \omega_0^2}. \quad (17)$$

If we assume that the coupling constant to position is much weaker than the coupling constant to velocity ($c_u \ll c_x$) and that the coupling constant to position is much weaker than the damping coefficient of the set-point dynamics ($c_u \ll \alpha_u$), then the transfer function of the dynamic set-point model reduces to the one of the damped spring model.

Appendix E

In this appendix, I calculate the transfer function of the deterministic part of the damped spring model with position and velocity coupling (Eq. (8)). Setting $Q_x = 0$ and Fourier transforming leads to

$$-\omega^2 X + \alpha_x i\omega X + \omega_0^2 X = c_v i\omega(S - X) + c_p S.$$

The transfer function $T_{xs}(\omega)$ is given by

$$T_{xs}(\omega) \equiv \frac{X}{S} = \frac{c_p + i\omega c_v}{-\omega^2 + i\omega(\alpha_x + c_v) + \omega_0^2}. \quad (18)$$

By comparing Eq. (18) with Eq. (17), we can relate the parameters of this model to the dynamic set-point model

$$c_p = \frac{c_u \omega_0^2}{i\omega + \alpha_y + c_u}, \quad (19)$$

$$c_v = c_x. \quad (20)$$

References

- Amblard, B., Crémieux, J., Marchand, A. R., & Carblanc, A. (1985). Lateral orientation and stabilization of human stance: Static versus dynamics visual cues. *Experimental Brain Research*, *31*, 21–37.
- Chow, C. C., & Collins, J. J. (1995). Pinned polymer model of posture control. *Physical Review*, *52*, 907–912.
- Collins, J. J., & De Luca, C. J. (1993). Open-loop and closed-loop control of posture: A random-walk analysis of center-of-pressure trajectories. *Experimental Brain Research*, *95*, 308–318.
- Collins, J. J., & De Luca, C. J. (1995). The effects of visual input on open-loop and closed-loop postural control mechanisms. *Experimental Brain Research*, *103*, 151–163.
- Dijkstra, T. M. H., Gielen, C. C. A. M., & Melis, B. J. M. (1992). Postural responses to stationary and moving scenes as a function of distance to the scene. *Human Movement Science*, *11*, 195–203.

- Dijkstra, T. M. H., Schöner, G., & Gielen, C. C. A. M. (1994a). Temporal stability of the action-perception cycle for postural control in a moving visual environment. *Experimental Brain Research*, *97*, 477–486.
- Dijkstra, T. M. H., Schöner, G., Giese, M. A., & Gielen, C. C. A. M. (1994b). Frequency dependence of the action-perception cycle for postural control in a moving visual environment: Relative phase dynamics. *Biological Cybernetics*, *71*, 489–501.
- Dijkstra, T. M. H., & Crowell, J. A. (2000). The dynamic set-point model of human postural control during quiet stance. *Journal of Experimental Psychology: Human Perception and Performance* (submitted).
- Dijkstra, T. M. H. (2000). The statistics of center of pressure and center of mass during quiet stance. *Experimental Brain Research* (submitted).
- Edwards, A. S. (1946). Body sway and vision. *Journal of Experimental Psychology*, *36*, 526–535.
- Feynman, R. P., Leighton, R. B., & Sands, M. (1963). *The Feynman lectures on physics*. Reading, MA: Addison-Wesley.
- Gardiner, C. W. (1985). *Handbook of stochastic methods* (second ed.). Berlin: Springer.
- Giese, M. A., Dijkstra, T. M. H., Schöner, G., & Gielen, C. C. A. M. (1996). Identification of the nonlinear state space dynamics of the action-perception cycle for visually induced postural sway. *Biological Cybernetics*, *74*, 427–441.
- Gurfinkel, V. S., Ivanenko, Y. P., Levik, Y. S., & Babakova, I. A. (1995). Kinesthetic reference for human orthograde posture. *Neuroscience*, *68*, 229–243.
- Harris, C. M., & Wolpert, D. M. (1998). Signal-dependent noise determines motor planning. *Nature*, *394*, 780–784.
- Jeka, J. J., Schöner, G., Dijkstra, T., Ribeiro, P., & Lackner, J. R. (1997). Coupling of fingertip somatosensory information to head and body sway. *Experimental Brain Research*, *113*, 475–483.
- Jeka, J. J., Oie, K., Schöner, G., Dijkstra, T., & Henson, E. (1998). Position and velocity coupling of postural sway to somatosensory drive. *Journal of Neurophysiology*, *79*, 1661–1674.
- Kamen, E. W., & Heck, B. S. (1997). *Fundamentals of signals and systems using MATLAB*. Upper Saddle River, NJ: Prentice-Hall.
- Karlsson, A., & Lanshammar, H. (1997). Analysis of postural sway strategies using an inverted pendulum model and force plate data. *Gait & Posture*, *5*, 198–203.
- Lee, D. N., & Lishman, J. R. (1975). Visual proprioceptive control of stance. *Journal of Human Movement Studies*, *1*, 87–95.
- Lestienne, F. G., & Gurfinkel, V. S. (1988). Posture as an organizational structure based on a dual process: A formal basis to interpret changes in posture in weightlessness. In O. Pompeiano & J. H. J. Allum (Eds.), *Progress in brain research*, Vol. 76 (pp. 307–313). Amsterdam: Elsevier.
- Myung, I. J. (2000). The importance of complexity in model selection. *Journal of Mathematical Psychology*, *41*, 190–204.
- Newell, K. M., Slobounov, S. M., Slobounova, E. S., & Molenaar, P. C. M. (1997). Stochastic processes in postural center-of-pressure profiles. *Experimental Brain Research*, *113*, 158–164.
- Paulus, W. M., Straube, A., & Brandt, T. (1984). Visual stabilization of posture: Physiological stimulus characteristics and clinical aspects. *Brain*, *107*, 1143–1163.
- Peterka, R. J. (1999). Quiet stance center-of-pressure predicted by a simple feedback model of human postural control. *Gait & Posture*, *9*, S13.
- Press, W. H., Flannery, B. P., Teukolsky, S. A., & Vetterling, W. T. (1988). *Numerical recipes in C*. Cambridge, UK: Cambridge University Press.
- Riley, M. A., Mitra, S., Stoffregen, T. A., & Turvey, M. T. (1997a). Influences of body lean and vision on unperturbed postural sway. *Motor Control*, *1*, 229–246.
- Riley, M. A., Wong, S., Mitra, S., & Turvey, M. T. (1997b). Common effects of touch and vision on postural parameters. *Experimental Brain Research*, *117*, 165–170.

- Schöner, G. (1991). Dynamic theory of action–perception patterns: The “moving room” paradigm. *Biological Cybernetics*, *64*, 455–462.
- Steinhage, A., & Schöner, G. (1997). Self-calibration based on invariant view recognition: Dynamic approach to navigation. *Robotics and Autonomous Systems*, *20*, 133–156.
- Schöner, G., Dijkstra, T. M. H., & Jeka, J. J. (1998). Action–perception patterns emerge from coupling adaptation. *Ecological Psychology*, *10*, 323–346.
- van Asten, W. N. J. C., Gielen, C. C. A. M., & Denier van der Gon, J. J. (1988). Postural adjustments induced by simulated motion of differently structured environments. *Experimental Brain Research*, *73*, 371–383.
- Wang, M. C., & Uhlenbeck, G. E. (1945). On the theory of Brownian motion II. *Reviews of Modern Physics*, *17*, 323–342.
- Zatsiorsky, V. M., & Duarte, M. (2000). Rambling and trembling in quiet standing. *Motor Control*, *4*, 185–200.
- Zwillinger, D. (1989). *Handbook of differential equations*. Boston, MA: Academic Press.